Available online at www.sciencedirect.com
ScienceDirect
Trans. Nonferrous Met. Soc. China 19(2009) 1514−1519
Transactions of Nonferrous Metals Society of China
www.tnmsc.cn

Influence of Yb_2O_3 addition on microstructure and corrosion resistance of 10Cu/(10NiO-$NiFe_2O_4$) cermets

GAN Xue-ping(甘雪萍), LI Zhi-you(李志友), TAN Zhan-qiu(谭占秋), ZHOU Ke-chao(周科朝)

State Key Laboratory of Powder Metallurgy, Central South University, Changsha 410083, China

Received 10 August 2009; accepted 15 September 2009

Abstract: 10Cu/(10NiO-$NiFe_2O_4$) cermets doped with Yb_2O_3 were prepared by conventional powder metallurgy technique. The effects of Yb_2O_3 content and sintering temperature on the relative density, phase composition, microstructure of the sintered cermets and the corrosion resistance to Na_3AlF_6-Al_2O_3 melts were investigated by sintered density test, XRD analysis and SEM. $YbFeO_3$ phase, which distributes in the ceramics grain boundary as particles or film, is produced by the reaction between Yb_2O_3 and ceramics. The addition of Yb_2O_3 accelerates the sintering process of ceramics matrix, eliminates pores in the boundary and results in coarsened crystalline grain. The relative density of the cermets with about 1% (mass fraction) Yb_2O_3 sintered at 1 275 ℃ increases to above 95%. Addition of about 1.0% Yb_2O_3 can inhibit obviously the corrosion of $NiFe_2O_4$ grain boundary and Cu phase in Na_3AlF_6-Al_2O_3 melts.

Key words: 10Cu/10NiO-$NiFe_2O_4$ cermets; Yb_2O_3 addition; sintering densification; microstructure; corrosion resistance; aluminum electrolysis

1 Introduction

The use of inert anodes for replacement of consumable carbon anodes in Hall-Heroult aluminum electrolysis cells has been a technical and commercial goal for many decades. In the present process, when consumable carbon anodes are used, the anode product is CO_2. With an inert anode, the anode product is O_2. The basic requirements for an inert anode are: 1) low corrosion rate in molten cryolite, 2) ability to produce commercially pure aluminum, 3) good electric conductivity, 4) being thermally stable up to electrolysis temperature, 5) adequate resistance to thermal shock and 6) being economically feasible[1]. Recently, the materials studied as inert anodes mainly concentrated on the alloy and the cermets. $NiFe_2O_4$-based cermets, which possess not only low solubility of ceramic to molten cryo1ite, but also high electrical conductivity of metal, are very promising as inert anode for aluminum electrolysis[2−3]. However, there are selective solubility of metal phase and grain-boundary corrosion of the $NiFe_2O_4$-based cermets in molten cryolite, resulting in the penetration of electrolyte into the inert anode, the reduction of service life and the increase of impurity in metal Al[4]. Sintering additive is effective to improve the microstructure and properties such as relative density, electric conductivity and corrosion resistance to cryolite melts[5−6]. JIAO et al[7] reported a gradual improvement in sintered density for nickel ferrite products by addition of TiO_2 up to 1%. LIU et al[8] pointed out that addition of MnO_2 increased the sintering density of nickel ferrite and improved the corrosion resistance to molten cryolite. The refined grains and improved thermal shock resistance were also obtained in cermet samples containing MnO_2. TIAN et al[9] have gained that the addition of SnO_2 decreased the activation energy and improved the electric conductivity of $NiFe_2O_4$-based cermets. ZHANG et al[10] found that proper addition of Sm_2O_3 into $FeAl_2O_4$-based cermet leads to bigger crystal of $FeAl_2O_4$ phase, higher anti-oxidation and electric conductivity. XI et al[11] found that the addition of V_2O_5 into $NiFe_2O_4$-based cermets is beneficial to improving obviously corrosion resistance to molten cryolite. In the *x*Cu/$NiFe_2O_4$ cermets, proper Y_2O_3 could improve the wettability between Cu

Foundation item: Project(2008AA030501) supported by the High-tech Research and Development Program of China; Project(200733) supported by the Postdoctoral Science Fund of Central South University, China; Project(50721003) supported by the National Natural Science Foundation for Innovation Group of China

Corresponding author: ZHOU Ke-chao; Tel: +86-731-88836264; E-mail: zhoukc2@mail.csu.edu.cn

DOI: 10.1016/S1003-6326(09)60062-5

and $NiFe_2O_4$ phase and enhance the bending strength and the thermal shock resistance[12]. However, those additives mentioned above could not improve the microstructure and properties at the meantime.

In this study, the 10Cu/(10NiO-90$NiFe_2O_4$) cermets doped with Yb_2O_3 were prepared. The influence of Yb_2O_3 addition on phase composition, microstructure, relative density and corrosion resistance to molten cryolite was investigated.

2 Experimental

2.1 Preparation of 10Cu/(10NiO-$NiFe_2O_4$) cermets doped with Yb_2O_3

10Cu/10NiO-$NiFe_2O_4$ cermets doped with Yb_2O_3 (＜3%＝ were prepared by the conventional powder metallurgy method with raw materials (reagent grade) including copper powder, Fe_2O_3, NiO and Yb_2O_3. The mixture of Fe_2O_3 and NiO in the molar ratio of 1.35:1 was calcined in a muffle furnace at 1 200 ℃ for 6 h in air and then the 10NiO-$NiFe_2O_4$ ceramic powder was obtained. X-ray diffraction result of 10NiO-$NiFe_2O_4$ ceramics is shown in Fig.1. The synthesized 10NiO-$NiFe_2O_4$ ceramic powder, Cu and Yb_2O_3 powder were ground in the media containing dispersant and adhesive. The dried mixture was cold pressed into cylindrical blocks (*d*20 mm×40 mm) at the pressure of 200 MPa. Then the samples were sintered at 1 250−1 325 ℃ for 4 h in nitrogen atmosphere.

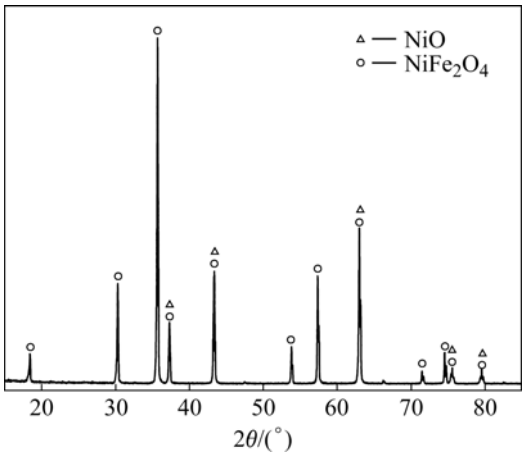

Fig.1 XRD patterns of 10NiO-$NiFe_2O_4$ ceramics

2.2 Characterization

The phase compositions were identified by X-ray diffraction analysis using Philips PW1390 X-ray diffractometer with Cu K_α radiation. Microstructure was analyzed by scanning electron microscope (SEM) (JSM-6360LV) and energy dispersive spectrometer (EDS) connected to the SEM. Bulk density and relative density were tested according to the Archimedes' method.

2.3 Electrolysis tests

The electrolyte was made up of Na_3AlF_6 and AlF_3 of reagent grade, CaF_2 and $A1_2O_3$ of technical grade; the CR (NaF/AlF_3 molar ratio) was 2.3; and the concentrations of CaF_2 and Al_2O_3 are both kept to be about 5%(mass fraction). All were added prior to electrolysis. The temperature was controlled at 960 ℃ with superheat of 10 ℃.

The sketch map of the experimental cell is shown in Fig.2. Alumina sleeve was set in the graphite crucible. About 400 g electrolyte was contained in the graphite crucible. The cell with the anode was placed in a vertical furnace and heated to the desired temperature and kept for 2 h before the anode was immerged into the electrolyte. The anode was immerged into the electrolyte by 20 mm. The current density of anode bottom was 1 A/cm^2 and the current was kept constant throughout the experiment, which lasted 10 h. By calculating the consumption rate of Al_2O_3 when cathode current efficiency was 85%, the concentration of Al_2O_3 in the bath decreased by 2.0% if Al_2O_3 was not added during the test. Moreover, alumina sleeve also contributes to keep the concentration of Al_2O_3. So, Al_2O_3 was not added into the bath during test. After electrolysis, the anode was raised out of the melt to prevent reduction of the anode material by dissolved metal aluminum. The cell was left to cool naturally with the anode resting above the electrolyte. The anodes tested were sectioned, polished, and analyzed by SEM (JSM−6360LV). The electrolyte after electrolysis test was analyzed by X-ray fluorescence spectrum (Philips 8424 TW2424) and the concentrations of Ni, Fe and Cu in electrolyte and

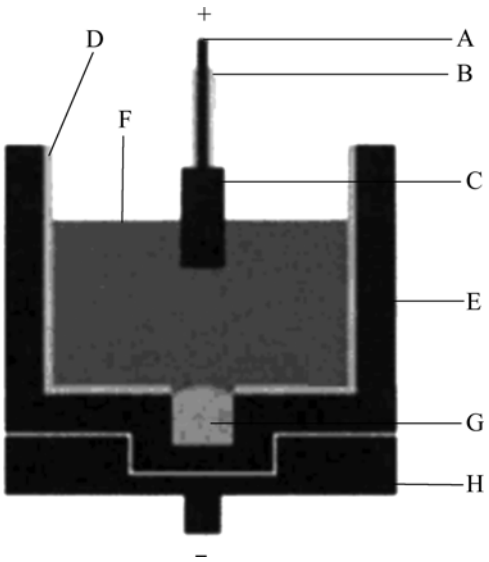

Fig.2 Sketch map of electrolysis experimental cell: A—Stainless steel anode rod; B—Al_2O_3 sleeve; C—Cermet inert anode; D—Al_2O_3 liner; E—Graphite crucible; F—Electrolyte; G—Metal aluminum; H—Graphite mechanical support

cathode aluminum were obtained, respectively.

3 Results and discussion

3.1 Phase composition and microstructure

The XRD patterns of 10Cu/(10NiO-$NiFe_2O_4$) samples doped with Yb_2O_3 and sintered at 1 275 ℃ are shown in Fig.3. It can be seen from Fig.3 that only $NiFe_2O_4$, NiO and Cu phases exist in the 10Cu/(10NiO-$NiFe_2O_4$) cermet samples. Besides the $NiFe_2O_4$, NiO and Cu phases, a new phase $YbFeO_3$ appeared in the 10Cu/(10NiO-$NiFe_2O_4$) cermet doped with 2.0% Yb_2O_3. However, Yb_2O_3 was not detected in the cermets doped with Yb_2O_3. This phenomenon indicates that the Yb_2O_3 in the sample has completely become $YbFeO_3$ in the sintering process. According to the phase diagram of Fe_2O_3-Yb_2O_3 system[13], the $YbFeO_3$ was possibly generated by the reaction:

$$NiFe_2O_4 + \frac{x}{2}Yb_2O_3 = NiFe_{2-x}O_{4-\frac{3x}{2}} + xYbFeO_3 \quad (1)$$

This reaction and formation of $YbFeO_3$ may lead to some Fe and O vacancies in the $NiFe_2O_4$ lattice.

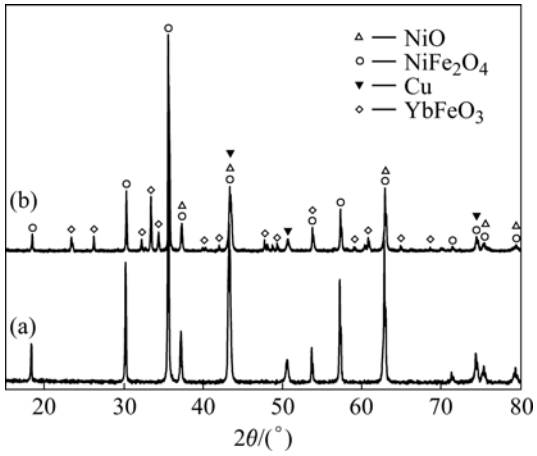

Fig.3 XRD patterns of 10Cu/(10NiO-$NiFe_2O_4$) samples sintered at 1 275 ℃: (a) Without Yb_2O_3; (b) With 2.0% Yb_2O_3

The SEM photograph of the polished surface of 10Cu/(10NiO-$NiFe_2O_4$) cermet doped with 2.0% Yb_2O_3 is shown in Fig.4. It can be seen that the $YbFeO_3$ phase distributed mainly along the $NiFe_2O_4$ grain boundary, which may be helpful for purification and strengthening of $NiFe_2O_4$ grain boundary.

The SEM photographs of the cermets sintered at 1 275 ℃ and doped with different contents of Yb_2O_3 are shown in Fig.5. It can be seen from Fig.5(a) that there are many pores in the sample without addition of Yb_2O_3 and the grain size is small, being 8−10 μm. As shown in Fig.5(b)−(d), the number of the pores in the sample decreased obviously and the grain size became large with the addition of Yb_2O_3 into 10Cu/(10NiO-$NiFe_2O_4$) cermets. In addition, tighter combination between the $NiFe_2O_4$ grains was achieved by addition of Yb_2O_3 to cermets due to removing of pores. This indicates that proper addition of Yb_2O_3 into 10Cu/(10NiO-$NiFe_2O_4$) cermets can accelerate the sintering process and improve properties of the cermets.

3.2 Effect of Yb_2O_3 addition on relative density of 10Cu/(10NiO-$NiFe_2O_4$) cermets

The relative densities of 10Cu/(10NiO-$NiFe_2O_4$) cermets doped with different contents of Yb_2O_3 sintered at 1 250−1 300 ℃ are listed in Table 1. It can be seen from Table 1 that the relative density of 10Cu/(10NiO-$NiFe_2O_4$) cermets sintered at 1 250 ℃ increased obviously with the addition of 0.5%−3% Yb_2O_3, which indicates that the presence of Yb_2O_3 in 10Cu/(10NiO-$NiFe_2O_4$) cermets could promote the sintering process. When the sintering temperature was 1 300 ℃, there was little difference in relative density with the increase of Yb_2O_3 content. It is possible that the presence of Fe and O vacancies in the 10Cu/10NiO-$NiFe_2O_4$ cermets, resulting from the formation of $YbFeO_3$, leads to more point defects in the material,

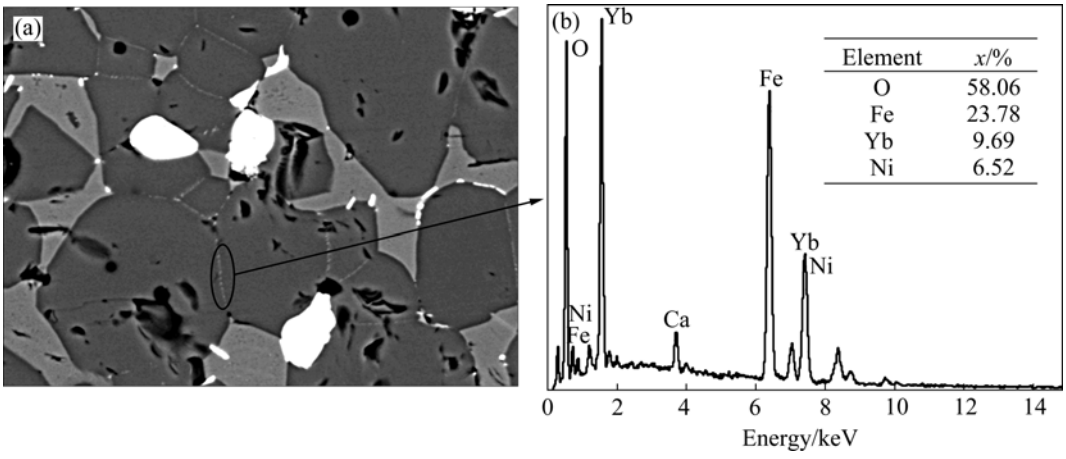

Fig.4 SEM photograph (a) and EDS (b) of 10Cu/(10NiO-$NiFe_2O_4$) cermets doped with 2.0% Yb_2O_3

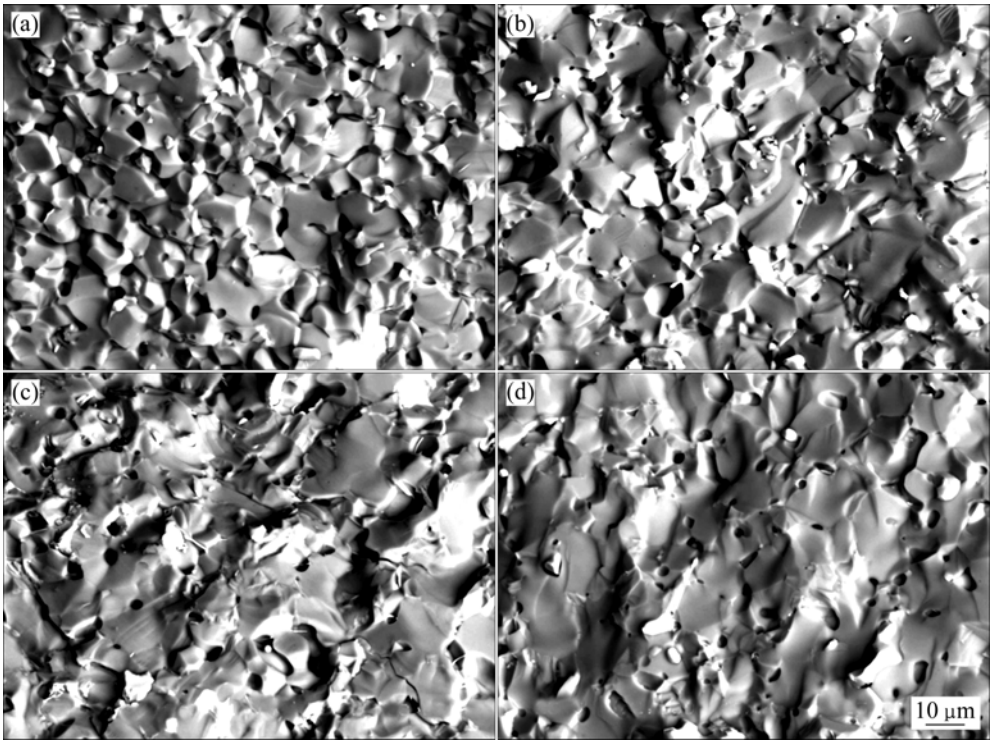

Fig.5 SEM fractographs of samples with different contents of Yb_2O_3: (a) Without Yb_2O_3; (b) 0.5% Yb_2O_3; (c) 1.0%Yb_2O_3; (d) 2.0%Yb_2O_3

Table 1 Relative densities of 10Cu/10NiO-$NiFe_2O_4$ cermets with different contents of Yb_2O_3

Content of Yb_2O_3/%	Relative density/%		
	1 250 ℃	1 275 ℃	1 300 ℃
0	86.92	93.16	94.40
0.5	89.75	95.58	94.89
1.0	90.62	94.85	95.23
1.5	88.42	95.72	94.74
2.0	89.99	95.42	95.06
3.0	91.82	94.76	93.51

helps the transportation of oxygen and Fe ions, and accelerates atomic diffusion and mass transportation, which finally promotes the sintering densification of 10Cu/(10NiO-$NiFe_2O_4$) cermets[14].

3.3 Corrosion resistance

LAI et al[15] pointed out that it took 5−6 h for the concentration of Cu, Ni or Fe in electrolyte during electrolysis test to reach steady state, which was about the solubility of Cu, Ni or Fe in the cryolite melts. Therefore, all electrolysis experiments lasted 10 h in this study. The concentration and mass change of Cu, Ni and Fe in electrolyte after electrolysis test are listed in Table 2. The results listed in Table 2 show that the steady-state concentration of Cu in the bath decreased from 0.0211% to 0.0178% as the Yb_2O_3 content changes from 0 to 1.0%, which is a little lower than its solubility (0.0226%) reported in the previous study[16]. The Yb_2O_3 addition has little effect on the concentration of Ni and Fe in the cryolite melts. The concentration of Ni was all close to the solubility (0.0125%) by LAI et al[16] (bath ratio 1.15, melt with 5% Al_2O_3, 965 ℃) and the concentration of Fe was all far lower than the solubility(0.0580%) mentioned by DEYOUNG[17] (bath ratio 1.1, melt with 6.5% Al_2O_3, 1 000 ℃). The total mass change of Cu, Fe and Ni in the electrolyte decreased from 0.90 to 0.774 g as the Yb_2O_3 content increased from 0 to 1.0%.

The content and mass change of Cu, Ni and Fe in metal aluminum after electrolysis test are listed in Table 3. It is obvious that the contents of impurities Cu, Ni and Fe in metal aluminum all decreased when 0.5% Yb_2O_3 was added into the 10Cu/(10NiO-$NiFe_2O_4$) cermets. More Yb_2O_3 addition has little effect on the impurities Cu, Ni and Fe in metal aluminum after electrolysis. This should be because the higher density of cermets inert anode by addition of Yb_2O_3 and the $YbFeO_3$ phases, which distribute in the $NiFe_2O_4$ grain boundary, could prevent the penetration of cryolite melt into the inert anode. In addition, the molar ratio of Fe to Ni in metal aluminum is 4.14−14.8, which is much more than that in cermets. That is to say, the transferring velocity of Fe from electrolyte to molten aluminum is more than that of Ni. This phenomenon is same with the results by

TIAN et al[4].

To obtain more information about the effect of Yb_2O_3 addition on the corrosion resistance to cryolite melt, the cermet inert anodes were sectioned, mounted and polished after electrolysis tests. The SEM photographs of anodes cross-section after electrolysis test are shown in Fig.6. According to Fig.6(a), the metal phase Cu is leached preferentially by cryolite melt, and there are many obvious holes and pores in the corrosion layer, which is about 200 μm after electrolysis test for 10 h. From Figs.6(b)and (c), it is found obviously that only less than 20 μm in the exterior surface of anodes was corroded when the 10Cu/(10NiO-$NiFe_2O_4$) cermets were added with 0.5% or 1% Yb_2O_3. By comparing Figs.6(a) with (b) and (c), the addition of Yb_2O_3 into 10Cu/(10NiO-$NiFe_2O_4$) cermets has improved obviously the corrosion resistance of the inert anode to the cryolite melts. This result corresponds with the content change of Cu, Ni and Fe in electrolyte and metal aluminum after electrolysis test.

Table 2 Concentration and mass change of impurities in electrolyte after electrolysis test

Yb_2O_3 content/%	w(Cu)/%	w(Ni)/%	w(Fe)/%	Δ(w(Cu)+ w(Fe)+ w(Ni))/%	Δ(w(Cu)+ w(Fe)+ w(Ni))/g
0	0.021 1	0.012 1	0.027 0	0.030 0	0.90
0.5	0.020 7	0.012 1	0.026 9	0.029 5	0.885
1.0	0.017 8	0.0117	0.026 5	0.025 8	0.774
1.5	0.018 1	0.012 3	0.027 7	0.027 9	0.837

Note: The concentrations of Cu, Fe and Ni in electrolyte before electrolysis were 6.6×10^{-5}, 1.95×10^{-4} and 4.1×10^{-5}, respectively

Table 3 Content and mass change of impurities in metal aluminum after electrolysis test

Yb_2O_3 content/%	m/g		w(Cu)/%	w(Fe)/%	w(Ni)/%	Δ(m(Cu)+m(Fe)+m(Ni))/g
	Before test	After test				
0	67.57	73.66	0.093 5	1.088 1	0.049 5	0.292
0.5	67.84	74.5	0.076 0	1.071 3	0.042 0	0.161
1.0	68.4	76.13	0.072 0	1.070 9	0.043 0	0.168
1.5	67.92	74.62	0.073 5	1.072 0	0.044 0	0.166

Note: Contents of Cu, Fe and Ni in metal aluminum were 5.8×10^{-5}, 1.68×10^{-3} and 3.6×10^{-5}, respectively

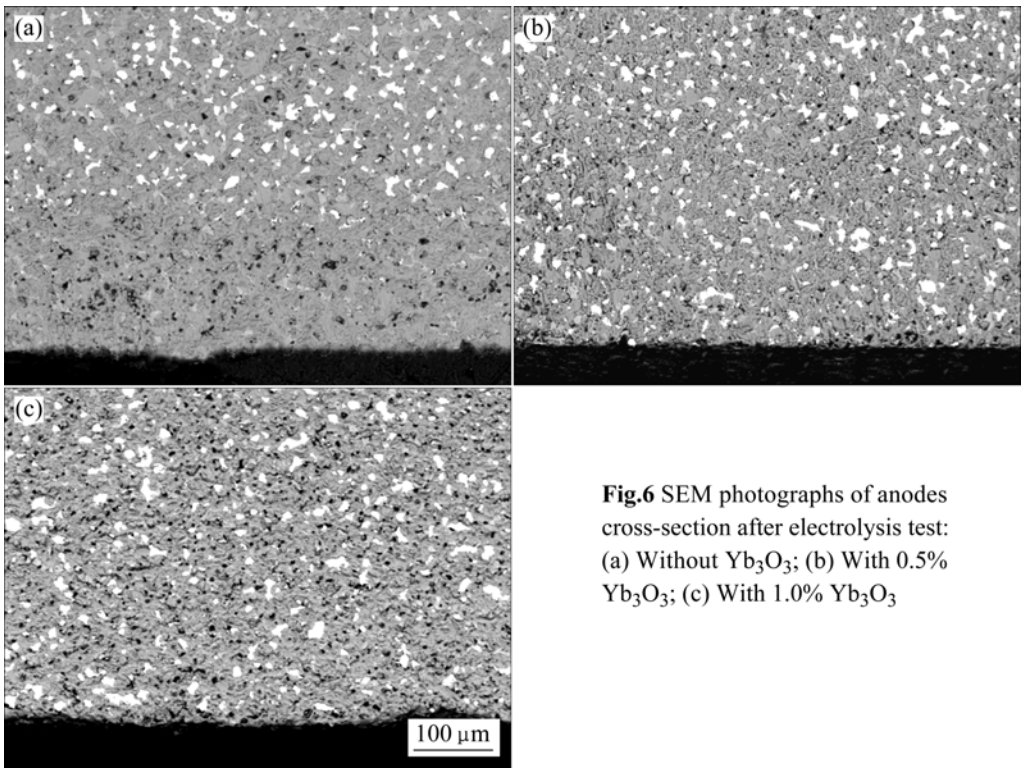

Fig.6 SEM photographs of anodes cross-section after electrolysis test: (a) Without Yb_3O_3; (b) With 0.5% Yb_3O_3; (c) With 1.0% Yb_3O_3

4 Conclusions

1) $YbFeO_3$ phase, which distributes in the ceramics grain boundary as particles or film, is produced by the reaction between Yb_2O_3 and ceramics when Yb_2O_3 is added to the 10Cu/(10NiO-$NiFe_2O_4$) cermets.

2) The addition of Yb_2O_3 accelerates the sintering process of ceramics matrix, eliminates pores in the boundary and results in coarsened crystalline grain. The relative density of the cermets with about 1% Yb_2O_3 sintered at 1 275 ℃ increases to 95%.

3) Proper addition of Yb_2O_3 and $YbFeO_3$ phase can inhibit the penetration of cryolite melts into the $NiFe_2O_4$ grain boundary, which improves the corrosion resistance of 10Cu/(10NiO-$NiFe_2O_4$) cermets inert anode to Na_3AlF_6-Al_2O_3 melts.

References

[1] OLSEN E, THONSTAD J. Nickel ferrite as inert anodes in aluminium electrolysis: Part I, Material fabrication and preliminary testing [J]. Journal of Applied Electrochemistry, 1999, 29: 293−299.

[2] KAENEL R V, NORA V D. Technical and economical evaluation of the de NORA inert metallic anode in aluminum reduction cells [C]// GALLOWAY T. Light Metals. Warrendale PA: TMS, 2006: 397−402.

[3] PAWLEK R P. Inert anode: An update [C]// TABEREAUX A T. Light Metals. Warrendale PA: TMS, 2004: 283−288.

[4] TIAN Zhong-liang, LAI Yan-qing, LI Jie, LIU Ye-xiang. Effect of Cu-Ni content on the corrosion resistance of (Cu-Ni)/(10NiO-$NiFe_2O_4$) cermet inert anode for aluminum electrolysis [J]. Acta Metallurgica Sinica, 2008, 21(1): 72−78.

[5] GAO Feng, LIU Xiang-chun, ZHAO Ming, LIU Jia-ji, TIAN Chang-sheng. Lattice structure and dielectric properties of Nd^{3+} doped (BaSr)TiO_3 ceramics [J]. Journal of the Chinese Rare Earth Society, 2007, 25(1): 59−63. (in Chinese)

[6] ZHOU Ke-chao, HE Han-bing, TAN Zhan-qiu, LI Zhi-you, GAN Xue-ping. Method for preparation of cermet anode material with high corrosion resistance to molten salt: CN200910304091[P]. 2009−07−08.

[7] JIAO Wan-li, ZHANG Lei, YAO Guang-chun, LIU Yi-han. Sintering process of $NiFe_2O_4$ spinel with and without TiO_2 adding [J]. Journal of the Chinese Ceramic Society, 2004, 32(9): 1150−1153. (in Chinese)

[8] LIU Yi-han, YAO Guang-chun, LUO Hong-jie, ZHANG Xiao-ming. Study on the nickel ferrate spinel inert anode for aluminum electrolysis [C]// GALLOWAY T. Light Metals. Warrendale PA: TMS, 2006: 415−420.

[9] TIAN Zhong-liang, LAI Yan-qing, DUAN Hua-nan, SUN Xiao-gang, ZHANG Gang. Effect of adding SnO_2 on electrical conductivity of nickel ferrite ceramics [J]. Conservation and Utilization of Mineral Resources, 2004(5): 37−40. (in Chinese)

[10] ZHANG Li-peng, YU Xian-jin, DONG Yun-hui, LI De-gang, LI Zhong-fang. Properties of cermets inert anode with adding rare earth oxide [J]. Journal of the Chinese Rare Earth Society, 2007, 25(2): 190−194. (in Chinese)

[11] XI Jing-hui, XIE Ying-jie, YAO Guang-chun, LIU Yi-han. Effect of additive on corrosion resistance of $NiFe_2O_4$ ceramics as inert anods [J]. Trans Nonferrous Met Soc China, 2008, 18(2): 356−360.

[12] WANG Chuan-fu, LI Guo-xun, QU Shu-ling, HUANG Ai-qin, LI Guo-bin. Influence of Y_2O_3 on the structure of the Cu-containing cermets[J]. Journal of Rare Earths, 1993, 11(3): 135−191.

[13] ROBERT S R, TAKI N, LAWRENCE P C. Phase diagrams for ceramists, Volume IV [M]. Cleveland: American Ceramic Society, 1981: 44.

[14] LIU Wei-yue, LIU Xiong-guang. The influence of sintering atmosphere on densification of ZTM/SiC composite[J]. Journal of Shanghai University, 1996, 29(5): 721−726. (in Chinese)

[15] LAI Yan-qing, LI Xin-zheng, LI Jie, TIAN Zhong-liang, ZHANG Gang, LIU Ye-xiang. Effect of metallic phase species on the corrosion resistance of 17M/(10NiO-$NiFe_2O_4$) cermet inert anode of aluminum electrolysis [J]. Journal of Central South University of Technology, 2006, 13(3): 214−218.

[16] LAI Yan-qing, TIAN Zhong-liang, QIN Qing-wei, ZHANG Gang, LI Jie. Solubility of composite oxide ceramics in Na_3AlF_6-Al_2O_3 melts [J]. Journal of Central South University of Technology: Natural Science, 2003, 34(3): 245−248. (in Chinese)

[17] de YOUNG D H. Solubilities of oxides for inert anodes in cryolite-based melts [C]// MILLER R E. Light Metals. DA: TMS, 1986: 299−307.

(Edited by YANG Hua)